Irreversible regional cerebral ischemia: serial MR imaging and proton MR spectroscopy in a nonhuman primate model.

L H Monsein, V P Mathews, P B Barker, C A Pardo, S J Blackband, W D Whitlow, D F Wong and R N Bryan

AJNR Am J Neuroradiol 1993, 14 (4) 963-970
http://www.ajnr.org/content/14/4/963

Irreversible Regional Cerebral Ischemia: Serial MR Imaging and Proton MR Spectroscopy in a Nonhuman Primate Model

Lee H. Monsein,[1] Vincent P. Mathews,[1] Peter B. Barker,[1] Carlos A. Pardo,[2] Stephen J. Blackband,[1] Warren D. Whitlow,[1,3] Dean F. Wong,[4] and R. Nick Bryan[1]

PURPOSE: To delineate the changes in proton MR spectroscopy and imaging that occur with acute, irreversible ischemia of the basal ganglia of a baboon. **MATERIALS AND METHODS:** The M1 segments of the middle cerebral arteries of six adult male baboons were occluded by endovascular means with microcatheters and N-butyl cyanoacrylate adhesive. Cerebral blood flow measurements were taken with positron emission tomography or radioactive microsphere techniques. Serial spatially localized proton MR spectroscopy of the basal ganglia and MR imaging of the brain were performed. The distribution of ischemic and infarcted tissue was demonstrated by histopathologic techniques or triphenyltetrazolium chloride staining. **RESULTS:** Radioactive microsphere or positron emission tomography measurements demonstrated no significant cerebral blood flow within the basal ganglia after occlusion of the middle cerebral artery. Proton MR spectroscopy of the basal ganglia demonstrated increasing cerebral lactate and decreasing N-acetyl aspartate within 30 minutes of middle cerebral artery occlusion. Changes in the MR imaging signal intensity of the basal ganglia were observed as early as 3.1 hours on T2-weighted, 3.3 hours on T1-weighted, and 6.1 hours on spin density–weighted images. The distribution of these changes correlated well with the histopathologic features of ischemia and infarction that were seen throughout the basal ganglia. **CONCLUSION:** Changes in MR imaging signal intensity corresponded to ischemia and infarction in our baboon model of acute irreversible ischemia of the basal ganglia. Increasing cerebral lactate and decreasing N-acetyl aspartate preceded changes in MR imaging signal intensity.

Index terms: Brain, ischemia; Basal ganglia, magnetic resonance; Magnetic resonance, spectroscopy; Magnetic resonance, comparative studies; Animal studies

AJNR 14:963–970, Jul/Aug 1993

Advances in stroke management will require techniques that allow the early and accurate diagnosis of cerebral ischemia and infarction. Magnetic resonance (MR) imaging and spectroscopy (MRS) have shown promise in evaluating patients with suspected cerebral ischemia (1–8), although data from early ischemia remain limited. These studies are noninvasive and can be performed with the same instrument in the clinical environment.

Atherosclerotic thromboembolic disease is the primary cause of acute cerebral infarction in adults. Over 50% of acute cerebral infarcts are caused by thromboembolic occlusions of the middle cerebral artery (MCA) (9). Early and severe ischemia and infarction of the basal ganglia may occur when there is occlusion of the MCA because the lenticulostriate artery branches of its M1 segment are "end vessels" without significant collaterals. Occlusion may be reversible, allowing reperfusion, or it may be irreversible.

In order to characterize the changes that are detectable with MR and proton MRS when there is acute, irreversible ischemia of the basal ganglia, we used a baboon model of MCA occlusion. Variable changes in cerebral blood flow (CBF), MR, proton MRS, and histopathology were ob-

Received February 28, 1992; revision requested June 18, received September 4, and accepted September 15.

Division of Neuroradiology[1] and Nuclear Medicine,[4] Russel H. Morgan Department of Radiology and Radiological Science, and Neuropathology Laboratory, Department of Pathology[2], Johns Hopkins University School of Medicine, Baltimore, MD 21205.

[3] Current address: Diagnostic Neuroradiology, PA, Dallas, TX.

Address Reprint Requests to Lee H. Monsein, M.D., Johns Hopkins Hospital, Meyer 8-141, 600 North Wolfe Street, Baltimore, MD 21205.

AJNR 14:963–970, Jul/Aug 1993 0195-6108/93/1404–0963

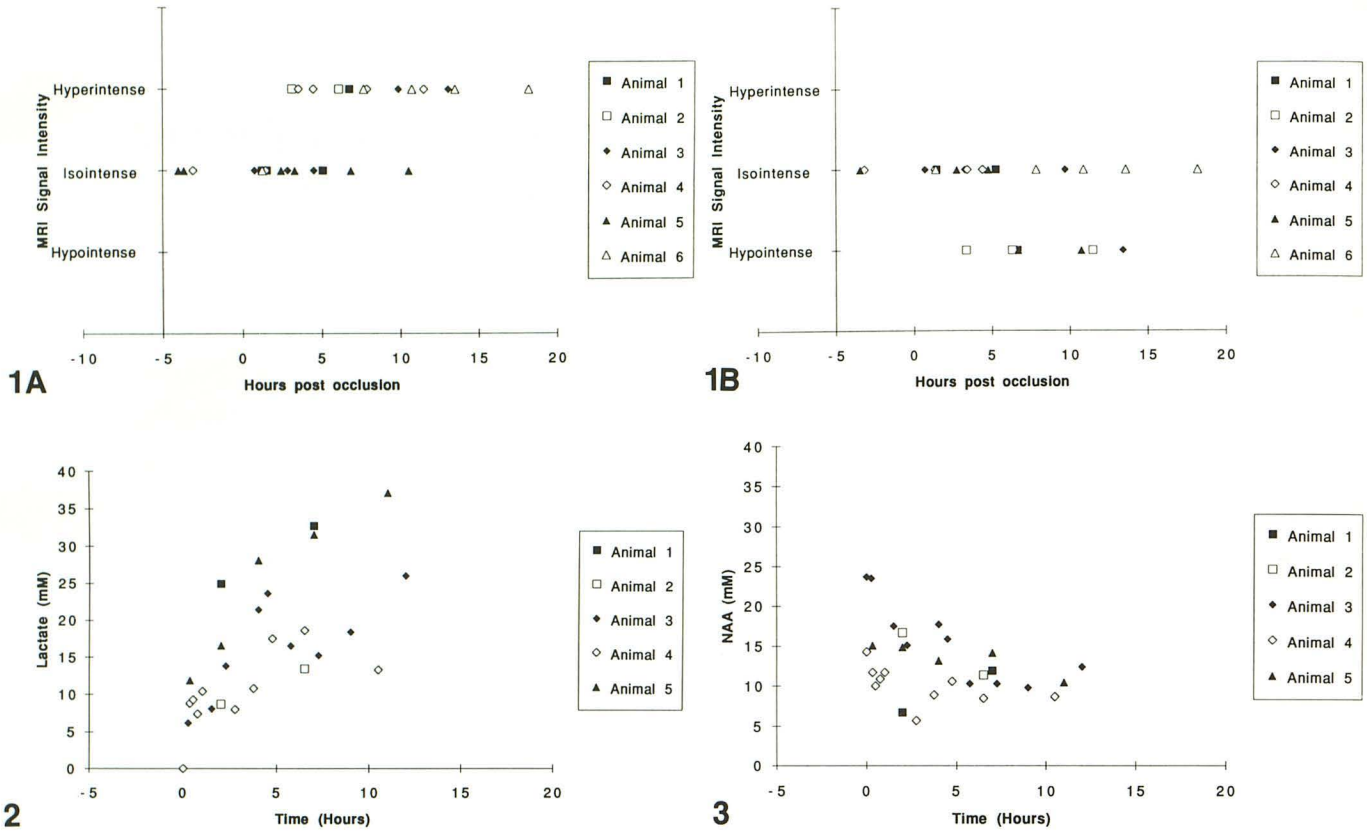

Fig. 1. Summary of MR signal changes.
A, Chart of T2-weighted signal changes.
B, Chart of T1-weighted signal changes.
Fig. 2. Summary of lactate concentrations.
Fig. 3. Summary of N-acetyl aspartate concentrations.

served throughout the ipsilateral hemisphere; however, this report will be limited to those related to the basal ganglia, where the CBF can be more uniformly controlled.

Methods

Animal Ischemia

After overnight fasting, six male baboons (16 to 18 kg) were anesthetized with alphaxalone (0.9%) and alphadolone acetate (0.3%; Saffan; Pitman-Moore, Ltd., Harefield, United Kingdom), which was initially administered intramuscularly (0.5 mg/kg) and subsequently intravenously (1 mL/kg per hour). Glycopyrrolate (Robinul; A.H. Robins Company, Richmond, Va; 0.1 mg/kg) was given intramuscularly to decrease pulmonary and salivary secretions. The animals were intubated, paralyzed with pancuronium (Pavulon; Organon, Inc., West Orange, NJ; 0.04 mg/kg) administered intravenously, and placed on a mechanical ventilator. A catheter was inserted into the bladder, and the abdomen was wrapped with a warm water-perfused blanket.

A 7-F sheath was placed in each common femoral artery. One was used for the placement of a left ventricular catheter, through which radiolabeled microspheres were injected for CBF measurements. The other was used for cerebral angiography or for the obtaining of reference blood samples for the CBF measurements.

Each animal was then transferred to a conventional MR scanner couch, and its head was positioned in a standard "extremity" radio frequency coil (Helmholtz saddle type of coil measuring 30 cm in length and 20 cm in diameter). All subsequent physiologic monitoring, angiography, MR, and proton MRS were performed without removing the animal from the couch or coil.

Oxygen saturation and electrocardiogram were monitored continuously during the experiment. End tidal-CO_2 concentration, arterial blood pressure, and body temperature were measured continuously when MR and MRS studies were not being performed. Oxygen tension, CO_2 tension, and pH of blood samples were measured intermittently. Blood glucose measurements were between 50 and 100 mg/mL at the beginning of the experiments.

A 7-F tapered to a 5-F catheter was introduced through one of the sheaths and was positioned in a common carotid

artery (CCA) under fluoroscopic guidance. A 2.0-F (Tracker 10) or a 2.7-F (Tracker 18) microcatheter (Target Therapeutics, Inc., Fremont, CA) was passed coaxially through the internal carotid artery (ICA) into the M1 segment of the MCA with a 0.010-inch or 0.014-inch guidewire. Digital subtraction angiography was performed when the tip of the catheter was in the ICA and the MCA. With the catheter in the MCA, a mixture of N-butyl cyanoacrylate adhesive, 500 mg of tantalum powder, and 0.5 mL of iophendylate (Pantopaque; Lafayette Pharmaceutical, Lafayette, IN) was injected until it was seen just exiting the tip of the microcatheter, which was then withdrawn. Digital subtraction angiography of the ipsilateral CCA was performed after occlusion of the MCA.

CBF Measurements

In three animals, the CBF was measured with radiolabeled microspheres (10) before the induction of ischemia, immediately after the acquisition of the first set of postocclusion images, and just before death. Approximately six million 15-μm radiolabeled microspheres (NEN-Trac, Dupont, NEN Research Products, Boston, MA) were injected through the left ventricular catheter while an arterial reference sample was simultaneously collected at 3.82 mL/min.

In the three remaining animals, a single postocclusion CBF measurement was obtained immediately before death by the use of positron emission tomography (PET) (11). $H_2{}^{15}O$ in a carrier solution of 5 to 8 mL of sterile saline was administered while arterial sampling was performed and an emission scan was acquired (Neuro ECAT PET; EG&G Ortec, Inc. Nashville, TN).

MR/MRS

MR and MRS data were obtained with a 1.5-T clinical MR instrument (Signa; General Electric Medical Systems, Inc., Milwaukee, WI). In two animals, MR imaging was performed before the induction of ischemia. In all animals, MR and MRS data were obtained at variable times (Figs. 1A and B, 2, and 3) after the induction of ischemia. Initial data were acquired as soon as possible after the induction of ischemia, which was dependent upon animal transport and stabilization time. The timing of subsequent data acquisition was determined by each animal's condition, instrument and personnel availability, and magnet shimming considerations.

MR consisted of contiguous sections, 5 mm thick, parallel or perpendicular to the anterior commissure–posterior commissure line with spin density–weighted 3000/30/1 (TR/TE/excitations), T2-weighted 3000/100/1, and T1-weighted 500/30/1 sequences. The signal intensity of the basal ganglia was categorized by a consensus of three readers (L.H.M., V.P.M., R.N.B.) as hypointense, isotense, or hyperintense relative to the unaffected contralateral basal ganglia.

Proton MRS spectra were recorded from the basal ganglia bilaterally using the stimulated-echo acquisition mode (STEAM) pulse sequence (12). Frequency selective single-lobe sinc pulses of 15-milliseconds' duration (13) were applied before and between the second and third section-selection pulses of the STEAM sequence for water suppression. Two hundred fifty-six scans (3000/270) were acquired with time mixing of 80 msec. Spectra were obtained from 8-cm^3 voxels, processed with 3-Hz line broadening, and analyzed by the use of a time domain nonlinear least squares fitting procedure (14).

Quantitation was performed with a fully relaxed water signal (10000/500, time mixing = 80) from the localized volume as an internal intensity reference (15). The water signal was corrected for the receiver attenuation value that was used to record it, and T1 and T2 relaxation times were measured from the double-echo MR images. Metabolite signal intensities were corrected for T1 and T2 losses, partial saturation effects caused by the water suppression pulses, and the number of protons per functional group. Concentrations were calculated assuming a cerebral water content of 80% and a tissue density of 1.049 g/cm^3 (16).

Pathology

All animals were euthanized 14 to 24 hours after the onset of ischemia.

In two animals, histopathologic analysis was performed. A catheter was passed into the left ventricle, the right atrium was incised, and the aorta was clamped distal to the left subclavian artery. Phosphate-buffered saline (0.1 mol/L, pH 7.4) was perfused for 10 minutes followed by 4% paraformaldehyde in 0.1 mol/L phosphate-buffered saline, pH 7.4, for 30 minutes. After perfusion, the brain was removed, postfixed in 4% paraformaldehyde for 48 hours, and cut in 5-mm-thick sections in a plane similar to that in which the MR images were obtained. The slices were cryoprotected in 20% glycerol for 48 hours and frozen in isopentane at −70°C.

Serial frozen sections (20 μm) were obtained and stained with cresyl violet, hematoxylin and eosin, and luxol-fast blue/hematoxylin and eosin. Cytologic criteria for necrotic cells included cytolysis, vacuolation, or nuclear condensation. Ischemic neurons were defined as cells with dendritic distortion, perikaryal-shape changes, and nuclear changes without condensation (17–21). The magnitude and topographical distribution of normal, ischemic, and necrotic neurons in each slide were determined, and a map was generated by the use of a computerized plotting system.

Three additional animals were euthanized with a lethal dose of intravenously administered potassium hydroxide immediately after a CBF measurement had been obtained by PET. The brain specimens were harvested, cut in sections 5 mm thick along the anterior commissure–posterior commissure line, and immersion stained with triphenyltetrazolium chloride (TTC) (22). Changes of ischemia or infarction were indicated by a lack of staining.

Results

Animal Ischemia

Baseline ICA angiography demonstrated bifurcation of the ICA into the MCA and anterior cerebral arteries. Selective angiography of the MCA (Fig. 4A) showed an "M1 segment" as in humans. CCA angiography after endovascular occlusion of the MCA with adhesive demonstrated a lack of opacification of the entire MCA (Fig. 1B).

CBF Measurements

Radioactive microsphere measurements demonstrated no significant CBF (<5 mL/100 g per min) in the ipsilateral basal ganglia in three animals after the first set of postocclusion images and at the completion of the experiments. $H_2{}^{15}O$ PET performed in the remaining three animals at the completion of the experiments demonstrated no significant CBF in the ipsilateral basal ganglia. Both techniques demonstrated preserved CBF in the contralateral basal ganglia.

MR/MRS

Changes in the MR signal intensity of the basal ganglia are detailed in Figure 1A and B. Abnormal signal intensity was seen as early as 3.1 hours after endovascular occlusion of the MCA on T2-weighted images, 3.3 hours on T1-weighted images, and 6.1 hours on spin density–weighted images. Signal intensity increased on the T2-weighted images of five animals. Signal intensity increased on the spin density-weighted images of two animals. In both cases, these changes were observed later than on the corresponding T2-weighted images. Signal intensity decreased on the T1-weighted images of three animals and did not change in the remainder. Figure 5 demonstrates a representative T2-weighted image of one animal with corresponding histopathology. Figure 6 demonstrates a representative T2-weighted image of another animal with a corresponding PET and TTC-stained specimen.

Proton MRS of voxels limited to the basal ganglia was performed in all animals, but the spectra from one animal were not interpretable because of technical difficulties with the spectrometer and a resulting poor signal-to-noise ratio. Representative spectra at several times for a single experiment are shown in Figure 7. The concentrations of lactate and NAA versus time for each animal are detailed in Figures 3 and 4. In general, the lactate concentrations increased and the NAA levels decreased over a similar time course. These changes consistently started before MR signal changes became apparent.

Pathology

Histopathologic analysis demonstrated ischemic and necrotic changes throughout the ipsilateral MCA territory (Figs. 5C and 5E) in contrast to the normal contralateral MCA territory (Figs. 5B and 5D). TTC revealed an absence of staining in the ipsilateral MCA territory (Fig. 6C).

Discussion

Reproducible animal models of regional ischemia that pathophysiologically resemble human clinical ischemia have been difficult to develop (23, 24). This is usually attributed to variability in surgical technique, vascular anatomy, and collateral blood supply. The anatomy of the MCA in the baboon offers a number of potential experi-

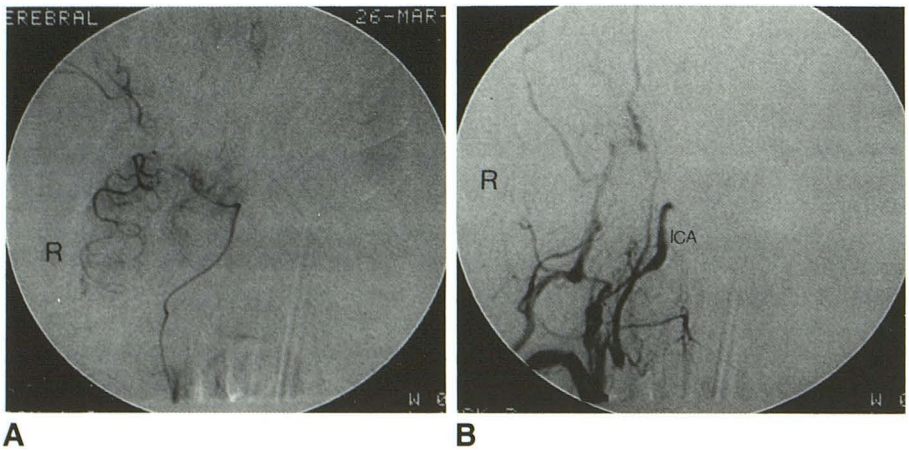

Fig. 4. Endovascular occlusion of the MCA in animal 6.

A, Digital substraction angiography of MCA (anteroposterior view) before occlusion.

B, Digital subtraction angiography of CCA (anteroposterior view) after occlusion demonstrating no opacification of the MCA.

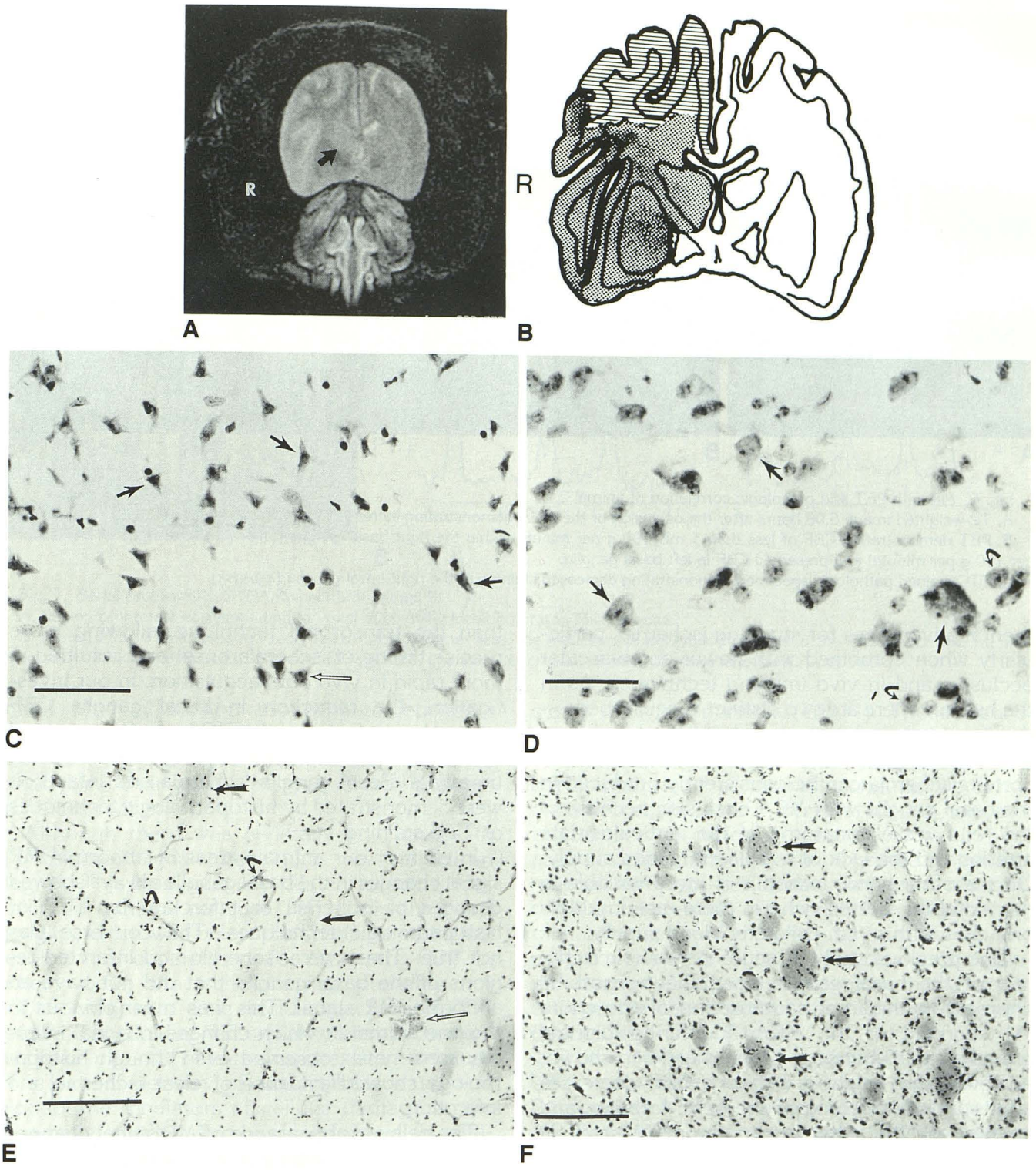

Fig. 5. MR with pathologic correlation of animal 4.

A, T2-weighted image 11.48 hours after occlusion of the MCA demonstrating mildly increased signal in the right basal ganglia (*arrow*).

B, Map of ischemia (*striped*) and infarction (*dotted*) generated from the plotting of microscopic changes. The former area is larger than that which demonstrates abnormal MR signal intensity.

C, Histologic preparation (cresyl violet) demonstrates ischemic (*open arrow*) and necrotic (*closed arrows*) neurons in the caudate. Note the shrinkage of neurons and pyknotic nuclei (bar = 5 μm).

D, Histologic preparation (cresyl violet) demonstrates normal large, medium (*arrows*), and small (*curved arrows*) neurons in the contralateral nonischemic caudate. Note the presence of identifiable nuclei, nucleoli, and cytoplasm (bar = 5 μm).

E, Histologic preparation (luxol fast blue/hematoxylin and eosin) demonstrates the presence of necrotic and ischemic neurons and the breakdown of the myelin tracts (*arrows*) in the basal ganglia. Hemorrhagic lesions (*open arrows*) and occluded blood vessels (*curved arrows*) are also present (bar = 25 μm).

F, Similar histological preparation (luxol fast blue/hematoxylin and eosin) of the nonischemic contralateral basal ganglia. Note the myelinization of the white matter tracts (*arrows*; bar = 25 μm).

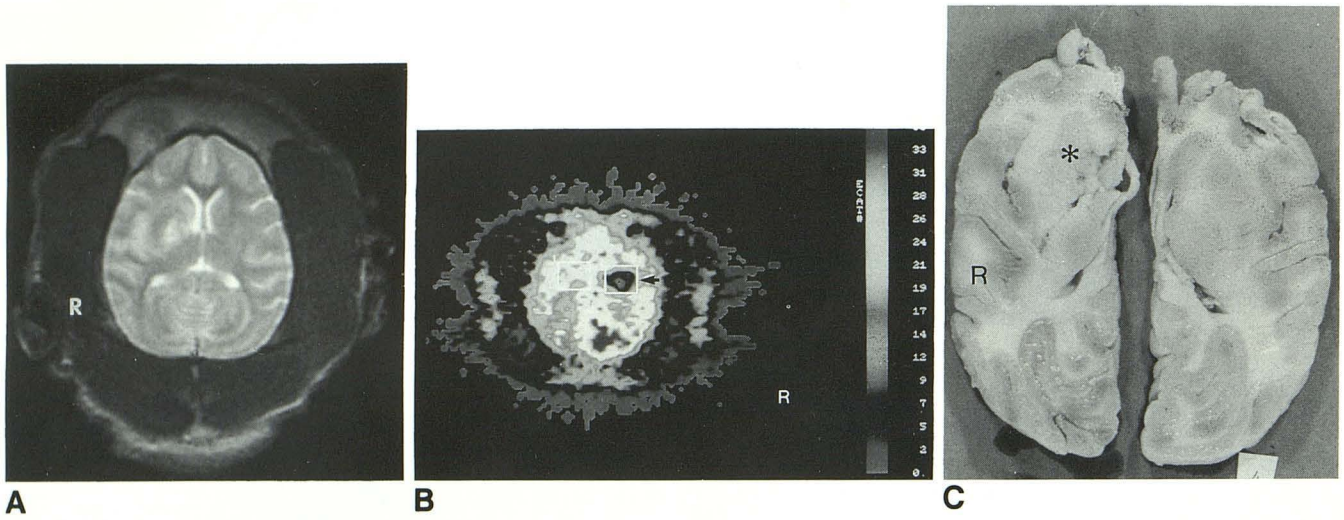

Fig. 6. MR with PET and pathologic correlation of animal 2.

A, T2-weighted image 6.08 hours after the occlusion of the MCA demonstrating increased signal in the basal ganglia.

B, PET demonstrating CBF of less than 5 mL/100 g per minute within the right basal ganglia (*arrow*; scale at right is in milliliters per 100 g per minute) and preserved CBF in left basal ganglia.

C, TTC-stained pathologic specimen demonstrating decreased staining in the right basal ganglia (*asterisk*).

mental advantages for studying ischemia, particularly when combined with newer endovascular occlusive and in vivo imaging techniques. As in the human, there are two distinct vascular beds—the proximal perforator supply to the basal ganglia and the peripheral branches to the cerebral cortex. Ischemia can be consistently produced in the basal ganglia with MCA occlusion because of the "end vessel" anatomy of the lenticulostriate arteries and the lack of a collateral blood supply. On the other hand, ischemia is more variable in the cerebral cortex where there are multiple branches with a rich collateral blood supply.

One previous study of acute irreversible ischemia of the basal ganglia used the transorbital approach with direct cauterization of the entire M1 segment of the MCA and lenticulostriate branches in 10 baboons (25). It has been shown, however, that in some baboons CBF decreases after surgical widening of the optic foramen and opening of the dura before the MCA itself is occluded (26, 27). This may be because of vessel spasm after the opening of the dura, leakage of cerebrospinal fluid, entrance of air into the subarachnoid space, or change of the surface temperature. In addition, data collection is delayed after transorbital occlusion, a major disadvantage for studying the critical initial phases of ischemia.

Brassel et al (26) previously demonstrated the effectiveness and irreversibility of the endovascular method we chose for occlusion of the MCA. This technique is much faster and less morbid than the transorbital technique, allowing more precise timing of ischemia onset and resulting in more rapid in vivo data acquisition. In our investigation, the reduction in basal ganglia CBF caused by occlusion of the MCA was documented by radioactive microsphere or $H_2{}^{15}O$ PET measurements. Basal ganglia ischemia and infarction were demonstrated by histopathologic techniques or TTC staining.

In each of our animals areas of abnormal MR signal changes in the basal ganglia always showed changes of ischemia or infarction by TTC or histopathologic techniques. The converse was not true. There were ischemic and infarcted regions of the basal ganglia that did not have an abnormal MR signal. This was most obvious in the one animal in which changes in signal intensity were never observed even though histopathology showed evidence of clear ischemia and infarction.

The delayed appearance of MR signal changes in the basal ganglia is consistent with prior clinical and experimental results. By the use of conventional spin-echo techniques, MR signal changes have not been reported earlier than 2 to 4 hours after ischemia (1–8). Our results indicate that ischemic changes are not appreciable on routine MR images until at least 3 hours after the ischemic insult, at which time changes in signal intensity were noted on T2-weighted images. Signal changes have been postulated to be caused by increased intracellular H_2O secondary to Na

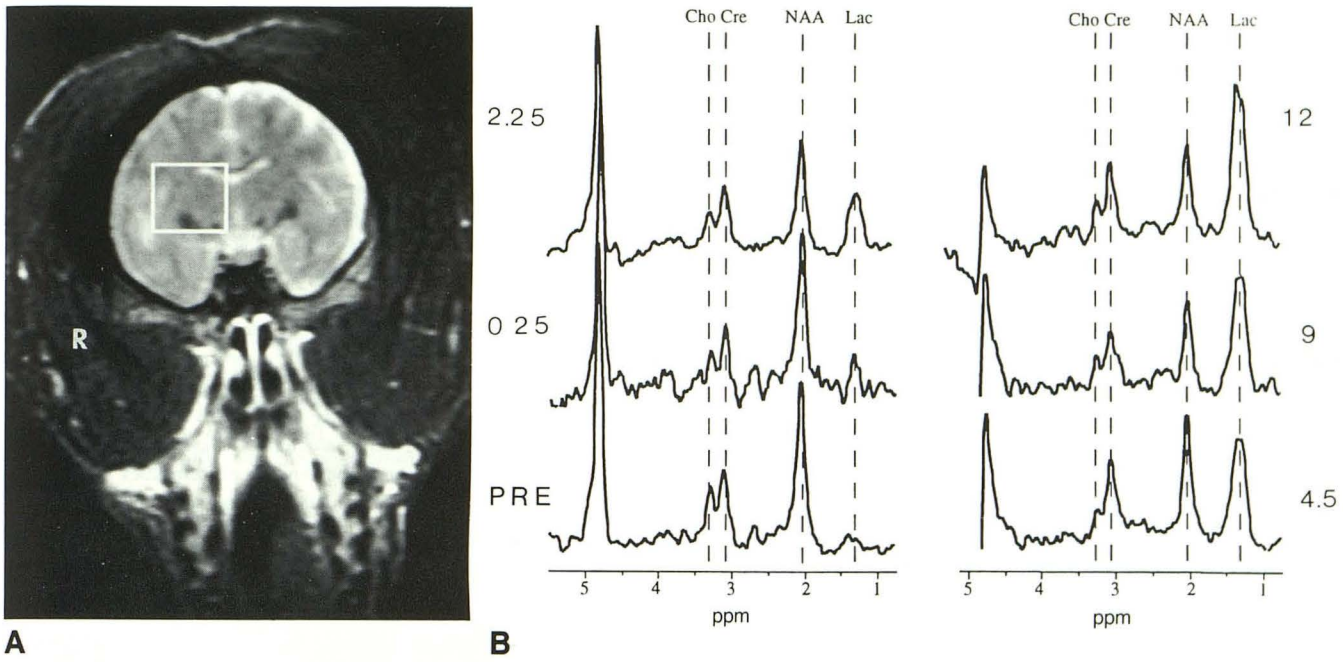

Fig. 7. Serial proton MRS STEAM spectra of animal 3.

A, Region of interest corresponding to voxel of spatially localized proton MRS spectra.

B, Proton MRS STEAM spectra recorded at multiple times after the induction of ischemia (numbers to the left of each spectra are the number of hours after occlusion). *Lac*, lactate; Cho, choline; Cre, creatinine; PRE, baseline before MCA occlusion.

influx after adenosine triphosphate-dependent Na/K pump failure (2, 6); however, it is possible that T2-weighted signal changes are caused by biophysical changes in water rather than changes in its concentration.

Although there was generally an increase in T2-weighted signal intensity, it was variable in degree. This was probably related to some variability in minimal residual CBF within the basal ganglia, which was below the spatial or statistical resolution of our methods for measuring CBF. In other words, the ischemia was probably not 100% "complete." One might expect that if CBF totally ceased, the MR signal intensity changes would be minimal or entirely nonexistent because of a lack of delivery of extracellular water and bloodborne mediators of cellular damage to the area being studied. We have performed an additional two experiments in which all vessels of the ipsilateral hemisphere were occluded with glue to decrease the chance for any residual CBF to occur; these experiments appear to lend support to this notion. In these animals, no change in signal intensity within the basal ganglia was ever seen (up to 24 hours after the onset of ischemia) (28).

Previous reports with animal models of global cerebral ischemia have described exponential increases in lactate concentrations with time constants of a few minutes (29–31). These results suggest that cell death is complete within 10 to 15 minutes of global ischemia. In contrast, with our animal model of regional ischemia, we demonstrated an increase in cerebral lactate concentration over a period of several hours. If one assumes that an exponential increase in lactate reflects complete cell death, perhaps a steadily rising lactate level in our model of regional ischemia indicates that cell death may not be universally complete throughout the volume of tissue we examined. This may also mean that there is salvageable tissue within this region of interest during this period of time.

Proton MRS showed a prolonged decrease in NAA, a postulated marker of viable neurons (12). Decrements of NAA were noted, however, before MR signal changes and coincident with increases in lactate. If NAA is indeed a reflection of neuronal viability, then the results suggest variable cellular agonal states, with some cells dying within minutes and other dying over a period of hours.

In conclusion, changes in MR signal intensity were always associated with cellular features of ischemia and infarction in our baboon model of acute irreversible ischemia of the basal ganglia. Sustained increases in cerebral lactate level and decreases in NAA preceded these changes in MR signal intensity by several hours. These early

changes in cerebral lactate and NAA may be useful clinical indicators of cerebral ischemia. They also suggest some variability in cellular viability within the basal ganglia and the potential opportunity of treatment regimens directed at salvaging cerebral tissue.

Acknowledgments

This work was supported in part by the American Society of Neuroradiology's Fellowship in Basic Science Research (L.H.M.), Radiology Society of North America's Research and Education Fund (V.P.M.), and the Fogarty International Fellowship (C.A.P.; #1 F05 TW 04305-01). We acknowledge the significant contributions of Elias K. Shaya (PET); Michael A. Samphilipo and Alex Y. Razumovsky (animal handling); and Cheryl L. Moser (MR imaging).

References

1. Spetzler RF, Zabramski JM, Kaufman B, Yeung HN. Acute NMR changes during MCA occlusion: a preliminary study in primates. *Stroke* 1983;14:185–191
2. Brant-Zawadzki M, Pereira B, Weinstein P, et al. MR imaging of acute experimental ischemia in cats. *AJNR: Am J Neuroradiol* 1986;7:7–11
3. Buonanno FS, Pykett IL, Kistler JP, et al. Cranial anatomy and detection of ischemic stroke in the cat by nuclear magnetic resonance imaging. *Radiology* 1982;143:187–193
4. Gyulai L, Schnail M, McLaughlin AC, Leigh JS Jr, Chance B. Simultaneous ^{31}P and ^{1}H nuclear magnetic resonance studies of hypoxia and ischemia in the cat brain. *J Cereb Blood Flow Metab* 1987;7:543–551
5. Horikawa Y, Naruse S, Tanaka C, Hirakawa K, Nisikawa H. Proton NMR relaxation times in ischemic brain edema. *Stroke* 1986;17:1149–1152
6. Kato H, Kyoka K, Ohtomo H, et al. Characterization of experimental ischemic brain edema utilizing proton nuclear magnetic resonance imaging. *J Cereb Blood Flow Metab* 1986;6:212–221
7. Levy RM, Mano I, Brito A, Hosobuchi Y. NMR imaging of acute experimental cerebral ischemia: time course and pharmacologic manipulations. *AJNR: Am J Neuroradiol* 1983;4:238–241
8. Moseley ME, Kucharczyk J, Montorovich J, et al. Diffusion-weighted MR imaging of acute stroke: correlation with T2-weighted and magnetic susceptibility-enhanced MR imaging in cats. *AJNR: Am J Neuroradiol* 1990;11:423–429
9. Olsen TS. Regional cerebral blood flow after occlusion of the middle cerebral artery. *Acta Neurol Scand* 1986;73:321–337
10. Heyman MA, Payne BD, Hoffman JI, Rudolph AM. Blood flow measurements with radionuclide-labeled particles. *Prog Cardiovasc Dis* 1977;20:55–79
11. Raichle ME, Martin WRW, Herscovitch P, Mintun MA, Markham J. Brain blood flow measured with intravenous $H_2{}^{15}O$-implementations and validation. *J Nucl Med* 1983;24:790–798
12. Frahm J, Bruhn H, Gyngell ML, Merboldt KD, Hanicke W, Sauter R. Localized proton NMR spectroscopy in different regions of the human brain in vivo. *Magn Reson Med* 1989;11:47–63
13. Haase A, Frahm J, Haenicke W, Matthei D. ^{1}H NMR chemical selection (CHESS) imaging *Phys Med Biol* 1985;30:341–334
14. Parker PB, Sibisi S. Non-linear least squares analysis of in vivo ^{31}P NMR data. Presented at the 9th Annual Meeting of the Society of Magnetic Resonance in Medicine, New York, NY, August 1990
15. Barker PB, Soher BJ, Blackband SJ, Chatham JC, Mathews VP, Bryan RN. Quantitation of proton NMR spectra of the human brain using tissue water as an internal concentration reference. *NMR Biomed* 1993;6:89–94
16. Narayana PA, Fotedar LK, Jackson EF, Bohan TP, Butler IJ, Wolinsky JS. Regional in vivo proton magnetic resonance spectroscopy of the brain. *Br J Magn Reson* 1989;83:44–52
17. Garcia JH, Kamijyo Y, Kalimo H, Tanaka J, Viloria JE, Trump BF. Cerebral ischemia: the early structural changes and correlation of these with known metabolic and dynamic abnormalities. In: Wishnant JP, Sandok BA, eds. Cerebral vascular diseases: Ninth Conference. New York: Grune & Stratton, 1975:313–328
18. Garcia JH, Lossinsky AS, Kauffman FC, Conger KA. Neuronal ischemic injury: light microscopy, ultrastructure and biochemistry. *Acta Neuropathol* 1978;43:85–95
19. Garcia JH. Morphology of global cerebral ischemia. *Crit Care Med* 1988;16:979–987
20. Garcia JH, Anderson ML. Physiopathology of cerebral ischemia. *CRC Crit Rev Neurobiol* 1989;4:303–324
21. Eke A, Conger KA, Anderson M, Garcia JH. Histologic assessment of neurons in rat models of cerebral ischemia. *Stroke* 1990;21:299–304
22. Bederson J, Pitts L, Germano S, et al. Evaluation of 2,3,5–triphenyltetrazolium chloride as a stain for detection and quantification of experimental cerebral infarction in rats. *Stroke* 1986;17:1304–1308
23. Hirschberg M, Hofferberth B. New model of cerebral thrombosis in dogs. *Stroke* 1988;19:741–746
24. Molinari GF. Experimental models of ischemic stroke. In: Barnett HJM, Stein BM, Mohr JP, Yatsu FM, eds. Stroke. New York: Churchill Livingstone, 1986:57–73
25. Wong DF, Solomon H, Natarajan TK, et al. Cerebral blood flow, oxygen and glucose metabolism in jeopardized cerebrum after experimental stroke (abstr). *J Nucl Med* 1988;29:852–853
26. Brassel F, Dettmers C, Nierhaus A, Hartman A, Solymost L. An intravascular technique to occlude the middle cerebral artery in baboons. *Neurology* 1989;31:418–424
27. Dettmers C, Hagendorff A, Nierhaus A, et al. Cerebral blood flow, tissue PO2, and somatosensory evoked potentials after intravascular occlusion of the middle cerebral artery in baboons. In: Meyer JS, Lechner H, Reivich M, Toole JF, eds. Cerebral vascular disease 7. Proceedings of the World Federation of Neurology 14th International Salzburg Conference. Amsterdam: Elsevier, 1988:229–237
28. Mathews VP, Monsein LA, Pardo CA, Bryan RN. *AJNR: Am J Neuroradiol* (in press),
29. Brown AW. Structural abnormalities in neurones. *J Clin Pathol* 1977;11:155–169
30. Rehncrona S, Rosen I, Siesjo BK. Brain lactic acidosis and ischemic cell damage: 1. biochemistry and neurophysiology. *J Cereb Blood Flow Metab* 1981;1:297–311
31. Siesjo BK, Wieloch T. Cerebral metabolism in ischemia: neurochemical basis for therapy. *Br J Anaesth* 1985;57:47–62